Heat Transfer in Fixed Beds at Very Low (<4) Tube-to-Particle Diameter Ratio

Anthony G. Dixon*

Department of Chemical Engineering, Worcester Polytechnic Institute, Worcester, Massachusetts 01609

New heat transfer measurements are reported for packings of full and hollow cylinders in tubes over a tube-to-particle diameter ratio (N) range of 1.8−5.6. Both high and low thermal conductivity packings were used. These results are analyzed in conjunction with previously-reported data for spheres in the range $1.13 < N < 6.4$ and data for cylinders and rings in the range $5.2 < N < 6.9$ to provide a comprehensive picture of heat transfer in the region of very low N (< 4) and a comparison to data at higher N. Single-phase heat transfer correlations are critically evaluated with regard to their dependence on N, to determine whether their range of applicability extends to $N < 4$. The effective radial thermal conductivity k_r and wall heat transfer coefficient h_w depend on N less strongly for full and hollow cylinders than they do for spheres. For spheres, there is evidence of high rates of radial heat transfer as N approaches unity, and the bed behaves as a single pellet string, but for $2 \leq N \leq 4$, k_r is highly dependent on the specific value of N.

Introduction

Fixed bed reactor tubes are often used in applications in which the need for the removal of heat from highly-exothermic chemical reactions (e.g., ethylene epoxidation to ethylene oxide) or the supply of heat to highly endothermic reactions (e.g., the steam reforming of methane to syngas) constrains the tube diameter to be small, but the need for high gas velocities and reasonable pressure drops constrains the particle diameter to be fairly large. The tube-to-particle diameter ratio, denoted here as N, following Borkink et al. (1993), can be quite small in these cases, usually in the range $4 \leq N \leq 10$, and sometimes as low as $N < 4$. Some laboratory studies of reacting systems have also been carried out at very low values of N (Kershenbaum and Lopez-Isunza, 1982; Vortmeyer and Winter, 1984).

The possibility of running fixed bed reactors at very low N has stimulated some investigators to address the question of whether pseudocontinuum models can still be used for such apparently discrete packing structures (Vortmeyer and Winter, 1984; Rao and Toor, 1984; Dixon and Yoo, 1992). Although the bed would appear to be far from a continuum at a given radial cross section, the averaging process in the axial direction that an element of fluid undergoes while passing through the longer tubes of industrial practice encourages the idea that pseudocontinuum models may give useful results down to quite low values of N. Recent work for beds of spheres (Dixon, 1994) suggests that fixed bed pseudocontinuum models are reasonable down to $N = 4$, in the sense that correlations can be found for the effective parameters in terms of N. Below $N = 4$, it was suggested that the discrete particle effects were too large, and no trends in the effective radial thermal conductivity ratio k_r/k_f and the wall Nusselt number Nu_w ($= h_w d_p/k_f$) could be discerned.

The use of constant values of k_r and h_w for fixed beds having quite large wall effects is possible if the parameters are correlated against a measure of the wall effects, such as N. One of the first such correlations was presented by DeWasch and Froment (1972). Since then there have been many approaches to this, including the correlation of individual-phase parameters against N and other process parameters and the combination of them to obtain the effective parameters (Dixon and Cresswell, 1979; Cresswell, 1986; Martin and Nilles, 1993). Very few correlations, however, extend to the region $N < 4$.

The work reported in this paper has been motivated by two considerations. First, since it is known that wall effects are reduced for full cylinders and hollow cylinders (rings) compared to those for spheres, it was desired to determine whether packings of cylinders and rings at $N < 4$ would be more amenable to the use of pseudocontinuum models. The possibility existed that effective parameters for cylinders and rings could be correlated against N under conditions where the large wall effects present in beds of spheres had previously precluded any systematic results. The experimental study reported here directly addresses that question. Second, it is conventional wisdom that as N decreases, the degree of bypassing at the wall increases and correspondingly poorer radial heat transfer rates will be observed. However, in studies of axial dispersion in packed beds of spheres in the range $1.1 \leq N \leq 2$ (Scott et al., 1974; Hsiang and Haynes, 1977) it has been suggested that qualitatively different behavior is observed for $N < 1.4$ and that radial cross-flow around particles could become significant. If this is so, it might be anticipated that such cross-flow could lead to high rates of radial heat transfer, thus reversing the usual trend with N. For this reason, it was decided to re-examine the data for spheres for very low N from previous studies (Dixon and Yoo, 1992; Dixon, 1994) and compare it to data in the present study for full and hollow cylinders at very low values of N to determine whether there is any possibility for good heat transfer and predictable behavior in this region.

Background

Studies of fixed bed structure, transport properties, and reactor behavior for tube-to-particle diameter ratios <4 have appeared sporadically in the literature. Only the topics of axial dispersion and, more recently, bed structure have seen any sustained development.

* Phone: (508) 831-5350. FAX: (508) 831-5853. E-mail: agdixon@wpi.wpi.edu.

S0888-5885(96)00595-7 CCC: $14.00 © 1997 American Chemical Society

The transient behavior of a fixed bed reactor of tube-to-particle diameter ratio $N = 3.1$ was studied by Kershenbaum and Lopez-Isunza (1982) for the partial oxidation of *o*-xylene to phthalic anhydride, and the same group has more recently reported on the difficulties of temperature measurement inside beds of such low N (Mongkhonsi et al., 1992). Steady-state experiments for reacting beds of $N = 2.1$ and $N = 2.8$ were reported by Vortmeyer and Winter (1984), for the catalytic oxidation of ethane. They were unable to obtain agreement between reactor model and data, which they ascribed to the highly-discrete nature of the bed, and concluded that continuum models would not be valid for such low ratios.

Some early, isolated results on radial transport of heat and mass have been published. Kunii et al. (1968) studied radial heat transfer in beds of Celite spheres of $N = 3.3$ and $N = 5.0$. An analysis of their results on effective radial thermal conductivity implies a value for the radial Peclet number, at large Re, of $Pe_r(\infty) = 8.3$, somewhat smaller than that predicted by most correlations. On the other hand, results for mass transfer (Olbrich and Potter, 1972b) and heat transfer (Olbrich and Potter, 1972a) at $N = 4.06$ yielded values of $Pe_r(\infty) = 16-19$, which was in good agreement with the literature correlation of Fahien and Smith (1955) which gave $Pe_r(\infty) = A(1 + 19.4/N^2)$ with A in the range 8−12. Chalbi et al. (1987) studied radial heat transfer for N between 3.29 and 18. The authors gave only the overall heat transfer coefficient at $N = 3.29$, since they could not obtain the individual parameters k_r and h_w in their narrower tubes.

The desire to use gas chromatography to measure diffusivities of porous particles leads to the requirement to use large particles so that the intraparticle diffusion is a significant contribution to the pulse spreading in the GC. Maintaining a large N would therefore lead to large GC tubes and a prohibitive gas flow volume requirement. Unfortunately, at smaller N the axial dispersion contribution to pulse spreading appears to increase. This led Scott et al. (1974) to the concept of the single-pellet-string reactor, which they investigated for $1.08 < N < 1.32$, and they showed that axial dispersion in this range intruded to the same extent as for high values of N and that the classical random walk limit of $Pe_a(\infty) = 2$ was obtained. Hsiang and Haynes (1977) confirmed this result for $N = 1.13$ and $N = 1.14$. Their other runs, in the range $1.54 \le N \le 8.19$, showed increased axial dispersion, which they attributed to mass transfer between the bed center gas stream and a fast-moving near-wall bypassing gas stream, a result which was confirmed later by the work of Ahn et al. (1986) for $N = 1.9$, 3.5, and 4.7. The latter workers also suggested that the pressure drop should be reduced for low-N beds. A variation on the single-pellet-string concept, in which a cylindrical particle is placed coaxially with the tube, has been reported by Schneider in a series of papers, the most recent of which gives results for $N = 1.50$ and presents an insightful review of the prior work in this area (Solcova and Schneider, 1994).

The second area in which extended work has been done for $N < 4$ is that of bed structure and void fraction. Benenati and Brosilow (1962) presented radial void fraction profile measurements for $N = 2.61$, while more recently McGreavy et al. (1986) used laser doppler velocimetry to measure velocity profiles in beds of $N = 3.1$, which they observed were not the same as velocity profiles measured above the bed. Dixon (1988a) has presented data and correlations for bulk void fraction for packings of spheres down to $N = 1.19$ and packings of cylinders and rings down to $N = 1.09$ (for nonspheres $N = d_t/d_{pv}$ where d_{pv} is the diameter of the sphere of equivalent volume). Chu and Ng (1989) used both experiments and computer-generated sphere packs to investigate fluid flow over the range $2.5 < N < 40$. Systematic studies of the bed structure have been developed in a series of papers begun by Govindarao and Froment (1986) for N values of 5.6 and above and more recently continued by Govindarao et al. (1992) with an exploration of the relation between bed structure and void fraction for $N < 2$. Mueller has presented theoretical and experimental work on the void fraction distribution for spheres with $N = 2.02$ and $N = 3.96$, in the radial (Mueller, 1992) and angular (Mueller, 1993) coordinates.

A systematic study of heat transfer in fixed beds of very low N (<4) is being pursued by the present author. The first set of experiments, using spheres in a nominal 3 in. column, yielded results in the range $1.70 \le N \le 3.96$ (Dixon and Yoo, 1992). From these results, it was concluded that continuum models of packed bed heat transfer could not represent radial temperature profiles for $N < 4$. This conclusion was based on the inability of the models that were evaluated in the study to fit the radial temperature profiles, on the basis of an analysis of variance F test. The measured angular-averaged radial temperature profiles showed extremely strong oscillations, especially in the near-wall region, that the models were unable to reproduce. In addition, the results for the dimensionless effective radial thermal conductivity k_r/k_f and the wall Nusselt number Nu_w, although plotting linearly with the Reynolds number Re for each individual packing, did not appear to vary with N in a systematic manner. The effect of N on k_r/k_f in particular was quite strong, but no trends were identifiable.

A follow-up study was performed to try to shed light on the reasons for the failure of the continuum models (Dixon, 1993). Fixed bed radial temperature profiles were measured at angular increments of 15° for spherical packings in a nominal 2 in. diameter tube, covering the range $1.14 \le N \le 14$. Angular temperature profiles were reported for the first time in beds of low N, as well as complete temperature contour plots for the bed cross section, for selected values of N. It was demonstrated that as N decreased, it became necessary to measure at an increased number of angular positions in order to obtain angular-averaged radial temperature profiles that were representative of the entire bed. If too few measurements were made, then oscillating radial temperature profiles were obtained, similar to those found in the earlier study. Measuring radial temperature profiles at angular increments of 45° was found to give averaged profiles that were not significantly different from those obtained by averaging radial profiles measured at smaller angular increments.

Following the study of angular variations, further work was carried out (Dixon, 1994) on heat transfer in packings of spheres, this time in the nominal 2 in. diameter column, over the range $1.14 \le N \le 4.0$, taking data at small enough angular increments to eliminate the oscillations seen in the original study. The two-dimensional pseudohomogeneous continuum model was able to fit nearly all of the experimental data well for $N \le 4$. In addition, the estimates of k_r/k_f and Nu_w from measurements spaced 45° apart were shown to be the

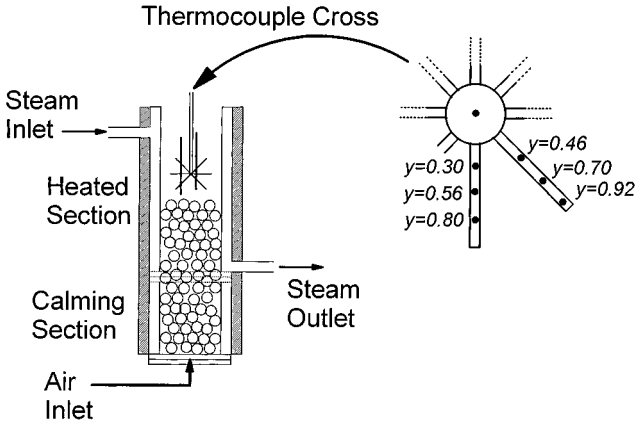

Figure 1. Schematic of heat exchanger column and thermocouple measurement cross.

same as those from more closely spaced measurements. It was also demonstrated that radial temperature profiles replicated at different angular positions, and radial temperature profiles at the same angular position but replicated over different repackings of the bed were equivalent. Additionally, the effective parameters estimated from angular replicates were the same as effective parameters estimated from repacking replicates. These results have also been extended to packings of full and hollow cylinders. Despite the improved model fits, and the fact that both k_r/k_f and Nu_w again correlated linearly with Re, no systematic trend with N was identifiable for either parameter, although the effect of N was clearly quite large for both. Thus neither experimental study was interpreted as giving results for the effective parameters in the range $N \leq 4$ that were amenable to correlation.

In the present work, the study of heat transfer in fixed beds of $N \leq 4$ is extended to packings of full and hollow cylinders, to determine whether the lesser influence of wall effects for these packings permits the influence of N to be more readily quantified. As a consequence of the work undertaken here, the results from the previous studies with spheres for $N \leq 4$ (Dixon and Yoo, 1992; Dixon, 1994) were re-examined together, and in comparison to higher N results, to obtain fresh insight into the effects of N and bed structure in the very low tube-to-particle diameter ratio region.

Experimental Apparatus and Procedure

The new experimental results reported in the present work were obtained for packings of full and hollow cylinders in columns of 50.8 mm (nominal 2 in.) and 26.2 mm (nominal 1 in.) diameters. The various combinations of packings and columns yielded results for the range $1.8 \leq N \leq 5.6$. Previous experimental work has reported results for packings of spheres, full cylinders, and hollow cylinders in the range $N > 5$ using a 75.4 mm (nominal 3 in.) column (Dixon, 1988b). Results have also been reported for packings of large spheres in the nominal 3 in. column giving $1.69 \leq N \leq 4$ (Dixon and Yoo, 1992) with the reservations noted above and for packings of spheres in the nominal 2 in. column giving $1.14 \leq N \leq 4$ (Dixon, 1994).

The experimental apparatus in nearly all respects was similar to that used in the previous studies referred to above. A schematic of the nominal 2 in. column and the thermocouple cross is presented in Figure 1. A 152.4 mm (6 in.) length of 50.8 mm i.d. nylon tubing was connected to the 467 mm long, 50.8 mm i.d. brass column, as shown in Figure 1, via nylon/brass flanges. Nylon bolts were used to minimize wall conduction between the two pieces of tubing. The nylon section was unheated, but the brass section was enclosed in a steam jacket and was mounted vertically above the nylon section. The combined tubes provided a continuous length of packing from the unheated to the heated section and could be packed to various depths of heated length of packing. The air flow was filtered and metered via calibrated rotameters and then fed to the bottom of the unheated nylon section. The nylon section allowed the flow to develop prior to entry into the heated test section. The measured pressure drop was negligible from the bottom to the top of the packed bed, where the air exited to the lab.

Thermocouples were fixed through the wall of the heated section, flush with the inside surface, to measure the heated wall temperature. These thermocouples were positioned 50.8, 228.6, and 381.0 mm above the metal/nylon interface. Similarly, thermocouples inserted through the unheated nylon wall of the calming section allowed the measurement of the temperature profile in the calming section wall. These thermocouples were positioned 6.35, 15.9, 25.4, 76.2, and 127.0 mm below the metal/nylon interface. This profile was present due to the unavoidable conduction from the heated section to the unheated section and resulted in the air flow being somewhat preheated before entry into the intentionally heated section. This phenomenon, and the length effects it can induce on estimates of heat transfer parameters, have been thoroughly discussed in an earlier publication (Dixon, 1985). The temperature of the air entering the nylon calming section was also measured.

Radial temperature profiles in the gas exiting the top of the packing were measured by thermocouples held by a cross with their tips approximately 3−6 mm above the packing. The cross consisted of eight arms, each holding three thermocouples, as partially shown in Figure 1. One arm carried thermocouples at three radial positions, and its neighbor carried three thermocouples at three different radial positions. These two configurations then alternated around the cross. There were, therefore, 24 thermocouples in all, for the 2 in. column, providing four angular replicates at 90° intervals, at each of six radial positions. This arrangement, however, did not give a complete radial profile of six measurements at any one angular position. The radial thermocouple positions were at 7.6, 11.6, 14.2, 17.8, 20.4, and 23.2 mm from the bed centerline. One additional thermocouple ran down the center of the cross and measured the temperature at the bed center. The cross and thermocouple supports were all made out of nylon or other low-conductivity plastics to minimize conduction from the wall to the thermocouples (Dixon, 1985).

The setup for the nominal 1 in. column differed from that described above for the nominal 2 in. column only in the diameter of the column, being 26.2 mm instead of 50.8 mm. The wall thermocouples in both heated and unheated sections were in the same axial locations as those for the larger column. For the narrower tube, however, the design of the thermocouple cross had to be modified as only two thermocouples could be fitted onto a single arm of the eight-arm cross. One arm carried two thermocouples, the next arm two more at different radial positions, the next arm carried still two more, and the fourth arm the final two, all at different

radial positions. The other four arms repeated this pattern. For the nominal 1 in. column, therefore, there were 16 thermocouples in all, providing two angular replicates at 180° intervals, at each of eight different radial positions. The radial thermocouple positions in this case were at 3.0, 4.6, 6.6, 7.9, 9.1, 10.5, 11.2, and 11.9 mm from the bed centerline.

For a typical run, the steam was turned on to bring the column walls up to temperature (approximately 100 °C depending on pressure), and then the air flow was begun. The cross was lowered to its position just above the column packing. Temperatures were then monitored until steady state was achieved, usually in about 2 h. The steady-state temperatures were then recorded for the given air flow rate, packing bed depth, and angular position. A position corresponding to 0° had previously been marked on the top flange of the column. The cross was then rotated 45° counterclockwise, and after the temperatures stabilized (a few seconds only) a second set of readings was taken. For the nominal 1 in. column, to compensate for the smaller number of angular replicates in a single set of readings, the cross was further rotated 45° twice more, providing a total of four sets of readings. For both columns, a measurement at a given radial position was replicated by these procedures at angular intervals of 45° for a total of eight replicates. This approach was previously reported to give reliable angular-averaged temperature profiles (Dixon, 1993) and parameter estimates (Dixon, 1994).

For the nominal 2 in. column, radial temperature profiles were measured at bed heights of approximately 102, 152, and 203 mm above the start of the heated section. The data from all bed depths were fitted simultaneously using the models discussed in the following section. For the nominal 1 in. column, radial temperature profiles were obtained at bed heights of 51, 102, and 152 mm; however the data at $z = 51$ mm were extremely scattered and gave poor model fits. For this reason only the data from the two longer bed depths were fitted by the models to give the effective parameter results reported below.

A total of nine different full and hollow equilateral cylinder packings were used in this study. There were three full cylinder packings made of 9.5 × 9.5 mm aluminum, 12.7 × 12.7 mm aluminum, and 9.5 × 9.5 mm porous ceramic materials. The six hollow cylinder packings were 8 × 8 × 6 mm glass, 6 × 6 × 4 mm glass, 13 × 13 × 7 mm solid (nonporous) ceramic, 9.6 × 9.6 × 4.8 mm solid (nonporous) ceramic, 8 × 8 × 4 mm porous ceramic, and 9.6 × 9.6 × 4.8 mm aluminum materials. Further details of the characteristics of these and other packings were presented in Dixon (1988b). It should be noted that the voidages given there were determined for each packing in a nominal 3 in. diameter column and so do not apply to the present work in columns of different diameter.

Model Equations

The temperature field is described by a two-dimensional (in r and z) pseudohomogeneous model, under the steady-state, nonreacting conditions of the present study. Angular variations are not usually represented in such models, an exception being the study of Mongkhonsi et al. (1992), who examined the nonaxially symmetric intrusive effects of radially-inserted thermocouples. The radial transport of heat through the bed is represented by an effective radial conductivity k_r, and the experimentally-observed steep increase in temperature near the wall is lumped into a temperature jump at the wall and described by an apparent wall heat transfer coefficient h_w. If axial dispersion of energy is included and represented by an effective axial thermal conductivity k_a, the model equations in dimensionless form are as follows:

$$\frac{1}{Pe_a}\frac{\partial^2\theta}{\partial x^2} + \frac{1}{Pe_r}\left(\frac{\partial^2\theta}{\partial y^2} + \frac{1}{y}\frac{\partial\theta}{\partial y}\right) = \frac{R}{d_p}\frac{\partial\theta}{\partial x} \tag{1}$$

$$(\partial\theta/\partial y) + Bi\theta = Bi\theta_{wc}(x) \quad \text{at} \quad y = 1 \tag{2}$$

$$\partial\theta/\partial y = 0 \quad \text{at} \quad y = 0 \tag{3}$$

$$\theta \to 0 \quad \text{as} \quad x \to -\infty \tag{4}$$

$$\theta \to 1 \quad \text{as} \quad x \to \infty \tag{5}$$

which is termed the wall conduction (WC) model. This model includes the experimentally-measured calming section wall temperature profile $\theta_{wc}(x)$ to allow for the heat leaks into the calming section which typically cause the so-called "length-dependence" of the model parameters (Dixon, 1985). For the axial dispersion term, the axial Peclet number is estimated by the formula

$$\frac{1}{Pe_a} = \frac{1}{Pe_a(\infty)} + \frac{k_{as}/k_f}{RePr} \tag{6}$$

in which $Pe_a(\infty) = 2.0$. The values of the axial solid thermal conductivity can be obtained from the formula of Bauer and Schlünder (1978b). Note that Pe_a is not an estimated parameter in this model. The model equations must be solved numerically, using a cubic Hermite piecewise polynomial collocation method. The measured wall temperatures in both the calming and test sections were interpolated by cubic spline functions, and the interpolation function was used to supply values of $\theta_w(x)$ at the points required by the numerical method. The experimental data from the 2 and 3 in. columns were analyzed using this model. More recently, we have obtained an analytical solution to these equations with the axial dispersion term omitted, using a simple functional representation of θ_{wc}, termed the wall conduction plug flow (WCPF) model. The data for the 1 in. column were analyzed using this newer model.

Results and Discussion

The effective radial thermal conductivity and apparent wall heat transfer coefficient were estimated from the data using the WC/WCPF models. The parameter estimates are presented in dimensionless form, as k_r/k_f and Nu_w, in Figures 2−11, where they are plotted versus the Reynolds number Re. A straight line has been fitted to the data for each individual packing to assist in identifying trends. The results for spheres in Figures 2 and 3 were obtained using the nominal 2 in. column. Similar results for these data were reported in Dixon (1994), using the axially-dispersed plug flow model with no wall profile and a fitted effective axial thermal conductivity. The WC model effective parameter results given here can be directly compared to the later values for nonspherical packings. In Figures 4−11 for full and hollow cylinders, parameter values for $N < 3$ came in general from the nominal 1 in. column, and values for $3 < N < 5$ came from the nominal 2 in. column and represent new data for the present work. Parameter values for $N > 5$ represent refitting of data

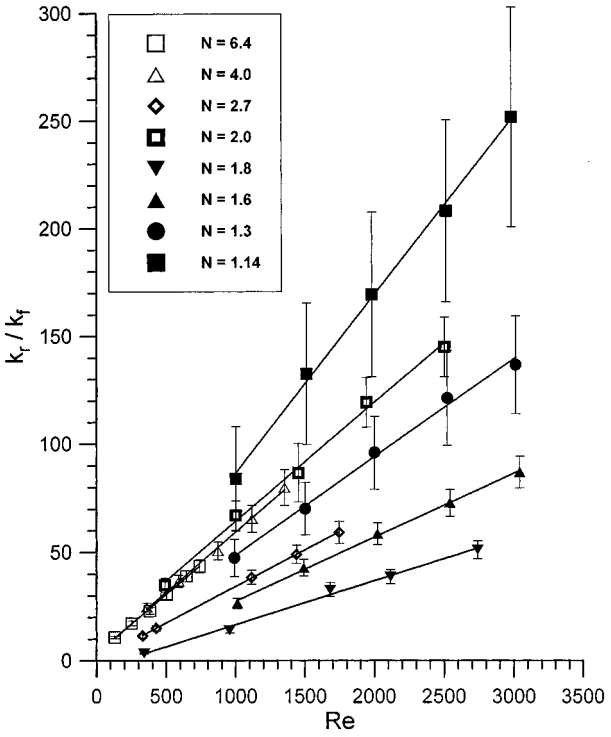

Figure 2. Effect of tube-to-particle diameter ratio N on effective radial conductivity k_r for beds of spheres (Dixon, 1994).

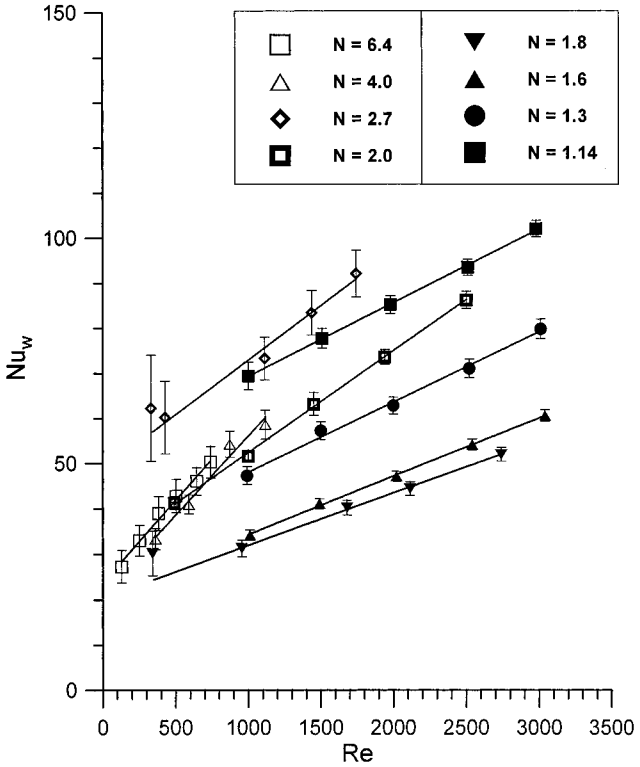

Figure 3. Effect of tube-to-particle diameter ratio N on wall Nusselt number Nu_w for beds of spheres (Dixon, 1994).

from a prior study (Dixon, 1988b) using the WC model and are included here as a basis for comparison to the new data. The only exceptions are in Figures 10 and 11 where the data for $N = 3.8$ came from the 1 in. column and the data for $N = 5.6$ came from the 2 in. column. All graphs show 95% marginal confidence intervals on the parameters, estimated using the angular replicates.

The k_r/k_f results for nylon/polystyrene spherical packings shown in Figure 2 exhibit a very wide spread of values. The results for $N = 6.4$ and $N = 4.0$ lie close together (and are also close to values for higher N, not shown here but see Dixon (1988b)). By comparison, lower k_r/k_f are seen for $N = 2.7$, and then the k_r/k_f for $N = 2.0$ are consistent with those from the higher N again, only for very low k_r/k_f values to be seen again at $N = 1.8$. There then appears to be a monotonic increase in k_r/k_f as N decreases from 1.8 to 1.14. To better delineate the different regimes, the values for $N > 4$, for which the influence of N is low, are plotted as thin-walled symbols. The values for $N < 2$ are plotted as full symbols, and the values for the intermediate range are plotted as thick-walled symbols. This representation is adhered to in the following Figures 3−11 as well. The k_r/k_f values plot linearly against Re, and their intercepts are reasonably consistent with the low stagnant thermal conductivity of the packing materials. The magnitudes of the k_r/k_f and their variation with N is in good agreement with earlier results (Dixon and Yoo, 1992) as will be discussed further below.

The Nu_w results for spheres shown in Figure 3 are not spread so widely as the k_r/k_f values, although a similar pattern emerges. For higher N, there is only a small effect of N, then a strong increase at $N = 2.7$, a decrease back to values consistent with the high-N results for $N = 2.0$, a strong decrease for $N = 1.8$, and then a monotonic increase as N decreases from 1.8 to 1.14. The values of Nu_w are well-represented by straight lines, although prior work would suggest that Nu_w should be proportional to $Re^{0.6-0.75}$ (Colledge and Paterson, 1984; Dixon and LaBua, 1985; Martin and Nilles, 1993) as Re increases. This apparent linearity may be due to the relatively narrow range of Re achievable in the experimental apparatus of this study. It is interesting that the confidence intervals for Nu_w are smaller than those for k_r/k_f, especially for the lowest N. The reason for this may be attributed to some very flat measured temperature profiles for low N (Dixon, 1994), which also have large temperature "jumps" near the wall, so that h_w is well-determined but k_r is not. The slopes of the lines fitted to the Nu_w data appear to decrease distinctly with decreasing N, and there also seems to be an effect on the intercept. These trends also will be discussed further below.

Figures 4 and 5 show the results for full aluminum cylinders. For k_r/k_f in Figure 4, the values are close in the range $3.5 \leq N \leq 6.9$, with only $N = 4.7$ a little lower than the others. There is then a fairly large decrease for $N = 2.4$ and $N = 1.8$, both in slope and intercept of the data. The decrease in intercept may be related to the increased void fraction for beds of cylinders in this range (Dixon, 1988a), while the lower values of k_r/k_f at higher Re may result from bypassing and thus reduced lateral mixing in these beds. Somewhat similar behavior is seen in Figure 5 for Nu_w, although there is actually little effect of N until $N = 1.8$. An indication of decreasing slope may be inferred from the data. Similar observations may be made in Figures 6 and 7 for packings of aluminum hollow cylinders. In this case, the data are all quite close for k_r/k_f, with those for $N = 3.5$ and $N = 2.4$ only a little lower than the others at higher N. For Nu_w, all the data are close, except for the results for $N = 5.2$, which appear to lie unexpectedly higher than the rest. Note that for these packings it was not possible to reach $N < 2$, where a stronger influence of N might be expected. All the high conductivity packings in Figures 4−7 give relatively high

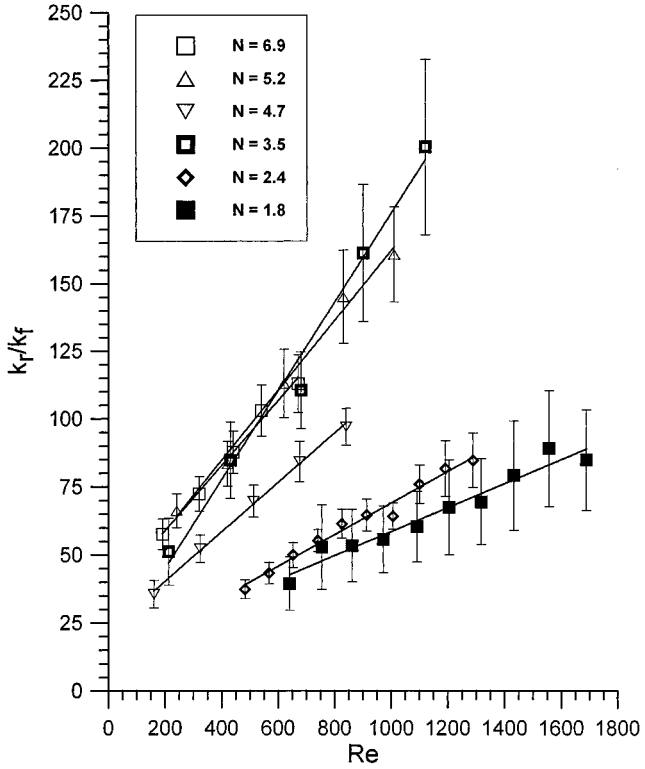

Figure 4. Effect of tube-to-particle diameter ratio N on effective radial conductivity k_r for beds of aluminum equilateral cylinders.

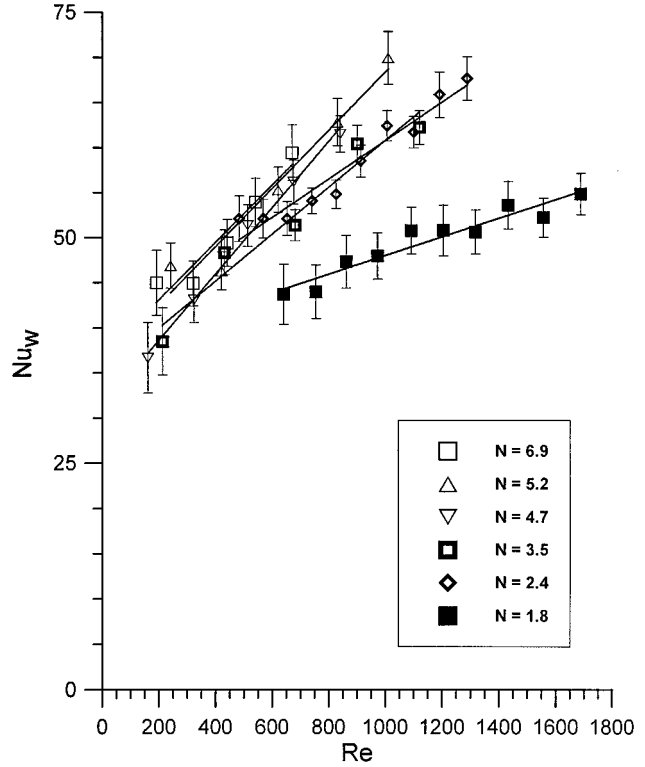

Figure 5. Effect of tube-to-particle diameter ratio N on wall Nusselt number Nu_w for beds of aluminum equilateral cylinders.

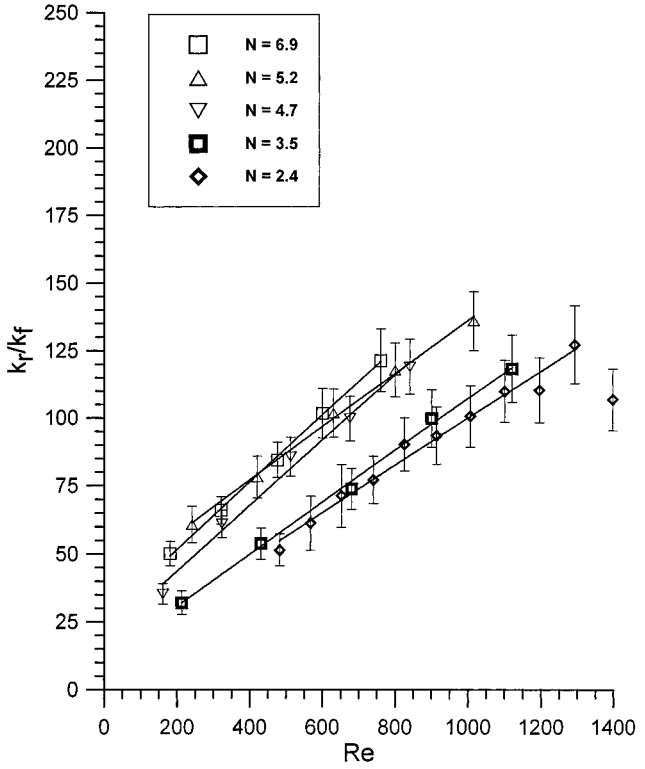

Figure 6. Effect of tube-to-particle diameter ratio N on effective radial conductivity k_r for beds of aluminum equilateral hollow cylinders.

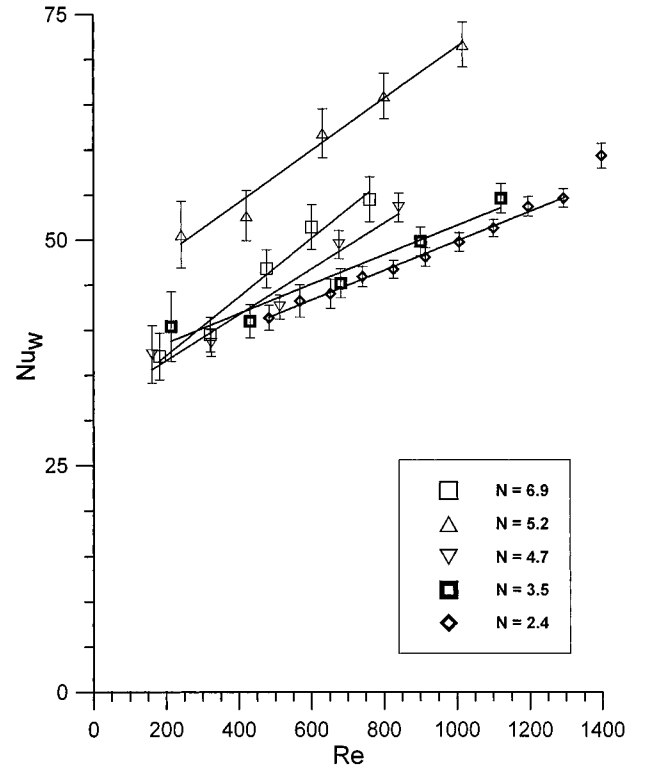

Figure 7. Effect of tube-to-particle diameter ratio N on wall Nusselt number Nu_w for beds of aluminum equilateral hollow cylinders.

intercepts at $Re = 0$, reflecting the effect of the particle conductivity on the stagnant bed contributions to k_r/k_f and Nu_w.

In Figures 8 and 9, results for nonporous ceramic hollow cylinders of moderate particle thermal conductivity are presented. In Figure 8, again, the results for k_r/k_f are close, with only those for $N = 1.8$ being significantly lower than the rest. Even this influence of N is muted for Nu_w, and a steady decrease in slope is seen in Figure 9 from $N = 6.9$ down to $N = 1.8$ with similar intercepts and no sudden drop in magnitude. For the porous ceramic full and hollow cylinders and glass hollow cylinders, the k_r/k_f values given in Figure 10 show only a minor effect of N, while the results for Nu_w in Figure 11 show that N has almost no effect. Only

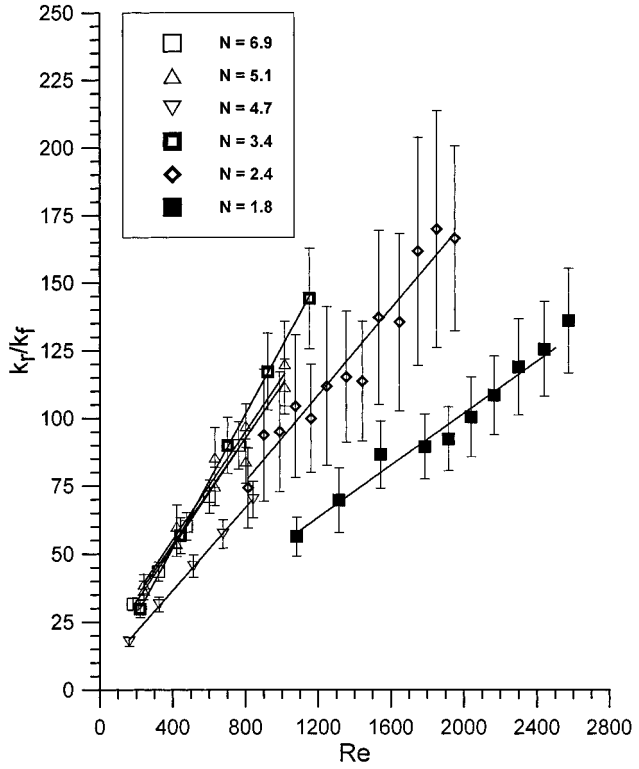

Figure 8. Effect of tube-to-particle diameter ratio N on effective radial conductivity k_r for beds of solid (nonporous) ceramic hollow cylinders.

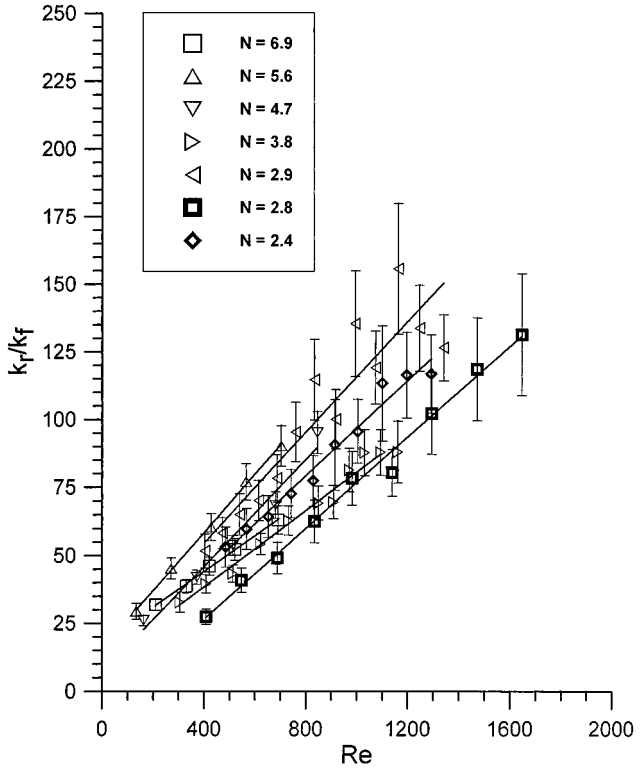

Figure 10. Effect of tube-to-particle diameter ratio N on effective radial conductivity k_r for beds of porous ceramic full and hollow cylinders and glass hollow cylinders.

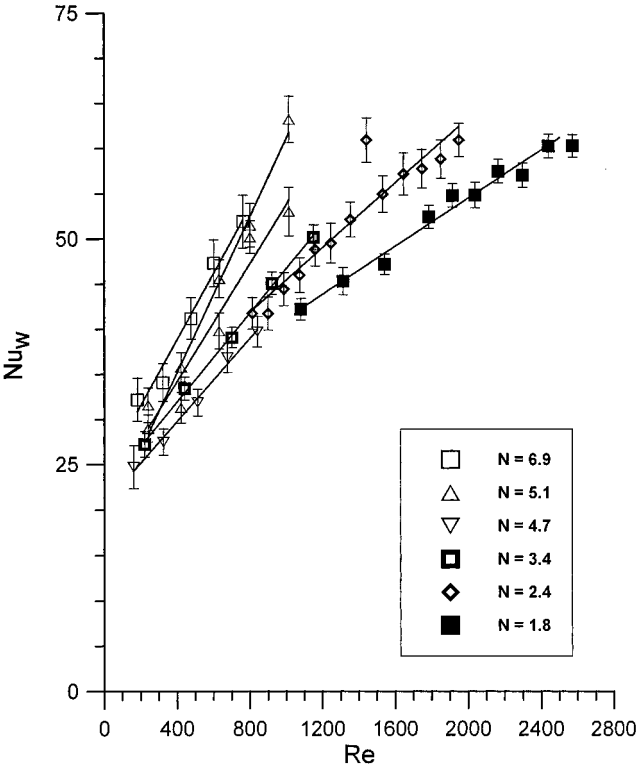

Figure 9. Effect of tube-to-particle diameter ratio N on wall Nusselt number Nu_w for beds of solid (nonporous) ceramic hollow cylinders.

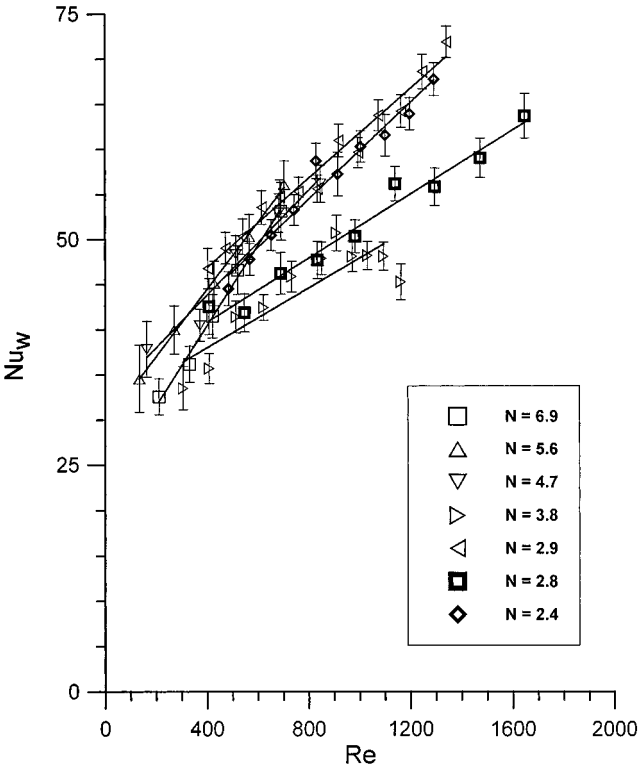

Figure 11. Effect of tube-to-particle diameter ratio N on wall Nusselt number Nu_w for beds of porous ceramic full and hollow cylinders and glass hollow cylinders.

the parameter values for $N = 2.8$ and $N = 3.8$ are somewhat lower than expected in comparison to those of the other packings, for both k_r/k_f and Nu_w. There is no apparent reason for this observation, except that it may be noted that these packings were both thin-walled glass rings, with larger internal void spaces than those with the other hollow cylinders, all of which had the internal diameter no larger than 50% of the external diameter. For the glass rings, the ratios were 67% ($N = 3.8$) and 75% ($N = 2.8$), and both packings had much larger bulk void fractions than those of the other packings.

Overall, the data presented in Figures 2−11 confirm and extend the trends reported earlier for packings in

the range $5 \le N \le 12$ (Dixon, 1988b). The ratio k_r/k_f is higher for higher conductivity packings and is dependent on particle shape, being higher for full and hollow cylinders than for spheres. The effect of N is minor, except in the very low range, and the data suggest that these are $N < 4$ for spheres and $N < 2$ for nonspheres. On the other hand, Nu_w is fairly insensitive to particle shape, but does appear to depend systematically on N over the range $1.8 < N < 7$, more strongly for spheres than for nonspheres. There is a minor effect of N on the intercept of Nu_w when it is correlated linearly against Re. Both k_r/k_f and Nu_w are well-correlated by a linear dependence on Re over the range studied.

The data presented in Figures 2−11 were all taken at $Re > 100$, and the majority were for $Re > 200$. In this range the high-Re formulas of Dixon and Cresswell (1979) apply, to relate the effective parameters to the underlying individual-phase phenomena, represented by the fluid-phase and solid-phase parameters. These formulas are as follows:

$$\frac{k_r}{k_f} = \frac{RePr}{Pe_{rf}(\infty)} + \frac{k_{rs}}{k_f}\frac{Bi_f + 4}{Bi_f}\left[\frac{8}{N_s} + \frac{Bi_s + 4}{Bi_s}\right]^{-1} \quad (7)$$

and

$$Nu_w = \frac{8}{N}\frac{k_{rs}}{k_f}\left[\frac{8}{N_s} + \frac{Bi_s + 4}{Bi_s}\right]^{-1} + Nu_{wf} + \frac{k_{rs}}{k_f}\left[\frac{8}{N_s} + \frac{Bi_s + 4}{Bi_s}\right]^{-1} Nu_{wf}\frac{Pe_{rf}(\infty)}{RePr} \quad (8)$$

written for the two dimensionless groups used in the present study.

For reasonably high Re, $8/N_s$ is small and we may accept the suggestion of Cresswell (1986) to take $Bi_f \approx Bi_s$ to obtain the *approximate* formula for k_r/k_f as the sum of a fluid- and a solid-phase contribution

$$\frac{k_r}{k_f} = \frac{RePr}{Pe_{rf}(\infty)} + \frac{k_{rs}}{k_f} \quad (9)$$

in which the solid conductivity term must be recognized as pertaining to the bed center, i.e., it must be estimated from data for which near-wall effects have been accounted for by an apparent wall-to-solid heat transfer coefficient. Similarly, since $Nu_{wf} \propto Re^{0.6-0.75}$, the third term on the right-hand side of eq 8 can be neglected for higher Re in comparison to the second to give an *approximate* formula for Nu_w, also as the sum of a fluid-phase and a solid-phase contribution

$$Nu_w = Bi_s\frac{k_{rs}}{k_f}\frac{2}{N} + Nu_{wf} \quad (10)$$

where the solid-phase Nusselt number Nu_{ws} has been rewritten in terms of a solid-phase Biot number.

If the approximate linear formulas of eqs 9 and 10 are applied to the data of Figures 2−11, they may be used to obtain estimates of the parameters $Pe_{rf}(\infty)$, Nu_{wf}, Bi_s, and k_{rs}/k_f. These may then be compared to the literature formulas for these parameters to determine whether they extend to the very low range, $N < 4$. It must be noted that some simplification has been carried out in obtaining eqs 9 and 10, and this and the degree of accuracy in the data indicated by the 95% confidence intervals should be kept in mind when the following results are interpreted.

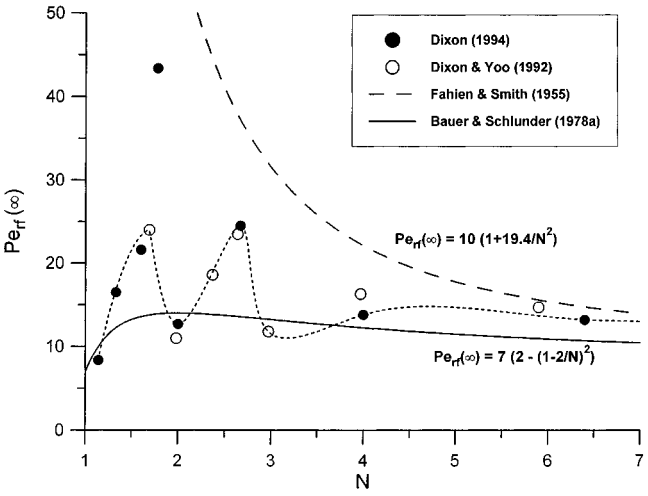

Figure 12. Comparison of two correlations for limiting fluid-phase radial Peclet number as a function of N to data for spheres from two prior studies.

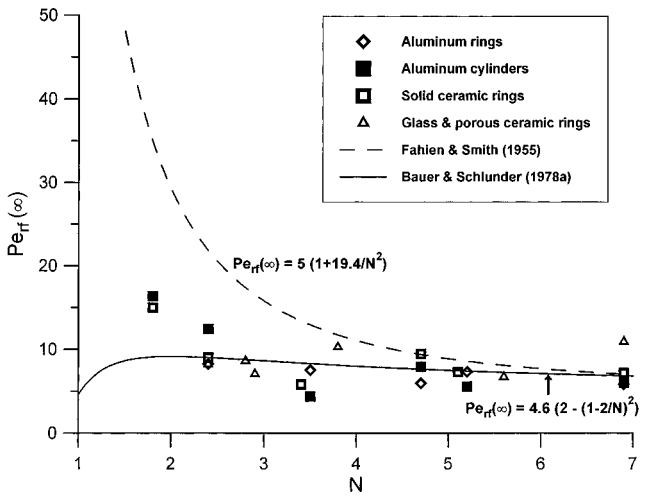

Figure 13. Comparison of two correlations for limiting fluid-phase radial Peclet number as a function of N to data for full and hollow cylinders.

Fluid-Phase Radial Thermal Conductivity. Values of $Pe_{rf}(\infty)$ were obtained from the slopes of straight-line fits to the data, using $Pr = 0.72$, and are presented in Figure 12 for the spheres data of Dixon (1994) and in Figure 13 for the nonspheres data of the present work. Also shown in Figure 12 are the values obtained from the spheres data of Dixon and Yoo (1992). Comparisons are made to two frequently-cited formulas for $Pe_{rf}(\infty)$ as a function of N. The first is the early work due to Fahien and Smith (1955)

$$Pe_{rf}(\infty) = A\left(1 + \frac{19.4}{N^2}\right) \quad (11)$$

where in Figure 12 an average $A = 10$ was used for spheres and in Figure 13 $A = 5$ was used for nonspheres. The second formula is due to Bauer and Schlünder (1978a)

$$Pe_{rf}(\infty) = A\left(2 - \left(1 - \frac{2}{N}\right)^2\right) \quad (12)$$

where $A = 8d_{pv}/x_F$ and the values of x_F, which depend on particle shape, are given in the original reference. The data of Figures 12 and 13 clearly show that, for very low N, the strong upturn in $Pe_{rf}(\infty)$ predicted by

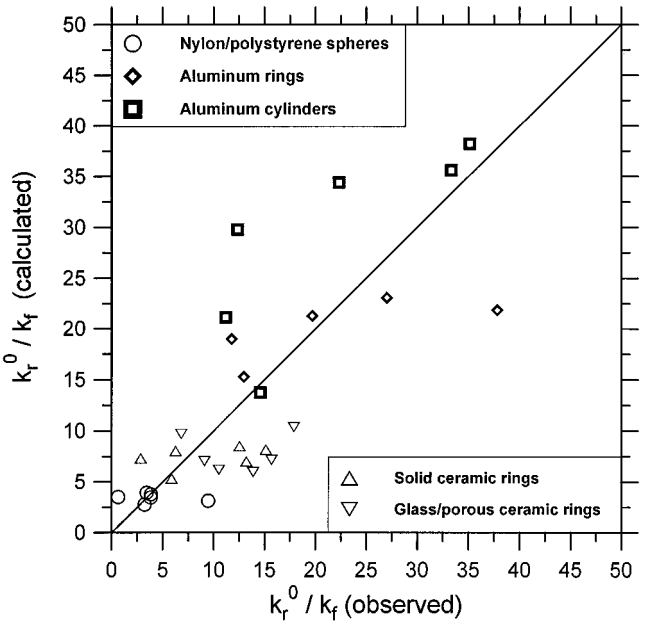

Figure 14. Parity plot for values of static effective radial thermal conductivity predicted by a formula of Bauer and Schlünder (1978b) and values extrapolated from flowing fluid data.

eq 11 is not supported. The Fahien and Smith (1955) formula was, however, developed empirically from data for spheres with $N > 6$ only, and it is unreasonable to expect it to extrapolate well beyond the conditions for which it was developed. The formula of Bauer and Schlünder (1978a) provides a better representation of the data, especially for nonspheres.

The behavior of $Pe_{rf}(\infty)$ for very low N for spheres in Figure 12 is worthy of special attention. As N decreases from 7 to 4, $Pe_{rf}(\infty)$ increases (k_{rf} decreases) as expected, due to the increased bypassing of flow along the wall, as the void fraction also increases. At $N = 3$, there is an unexpected low value of $Pe_{rf}(\infty)$, followed by higher values between 3 and 2, another low value at $N = 2$, high values for N slightly below 2, and then decreasing values as N decreases from 2 toward 1. This pattern is emphasized by the dotted curve in Figure 12. Data from both studies using different tubes are in good agreement, with only a single data point departing from the pattern. An explanation for this behavior may be found by consideration of the packing of spheres in a tube at very low N. At $N = 3$, a distinguished packing state can exist, in which the spheres stack in such a way as to "block" any paths for fluid bypassing, thus promoting good radial transport (high k_{rf}). The spheres can form a ring packed tightly against the wall, with room for a centerline sphere to sit in the middle of the ring. For $2 < N < 3$, the lower values of k_{rf} correspond to "holes" in the packing, as the spheres can pack either in a stable torus, leaving a pathway for flow bypassing down the center of the bed, or they can collapse into the bed center, leaving large pathways for flow bypassing at the wall, both arrangements thus reducing the radial displacement of fluid. This phenomenon, and temperature profiles associated with it, were demonstrated previously (Dixon, 1994). At $N = 2$, the spheres pack in pairs in alternating layers, thus creating another distinguished state. The centerline hole is closed up at $N = 2$, and each layer blocks the large near-wall void spaces of the preceding layer, to promote transverse movement of fluid. This results in the higher k_{rf}/lower $Pe_{rf}(\infty)$ values seen. Immediately below $N = 2$, the spheres must pack in a staggered single file, with large twisting paths for easy fluid bypassing. As N decreases from 2 to 1, the radial displacement to move around a sphere increases, promoting good radial heat transfer and smaller $Pe_{rf}(\infty)$ values. The Bauer and Schlünder (1978a) formula does quite well in predicting $Pe_{rf}(\infty)$ for those packings with high k_{rf}, i.e., with good radial displacement, but could seriously overestimate k_{rf} for the "in-between" packing states in which there is a high degree of flow bypassing. For nonspheres, there is no strong evidence of any distinguished states for $N > 2$, and only a couple of data points below $N = 2$ indicate any behavior similar to that of spheres.

Solid-Phase Radial Thermal Conductivity. The values of k_r^0/k_f obtained from linear extrapolation of the data to zero-flow conditions should represent bed-center values, as the wall heat transfer coefficient was estimated simultaneously. The formula of Bauer and Schlünder (1978b) was derived under similar conditions. Omitting terms relevant to low pressure and surface oxide effects gives

$$\frac{k_r^0}{k_f} = \frac{k_{rf}^0}{k_f} + \frac{k_{rs}}{k_f}$$

$$= (1 - \sqrt{1-\epsilon})\left(1 + \frac{k_R}{k_f}\right) + \frac{2\sqrt{1-\epsilon}}{1 - \frac{k_f}{k_p}B} \times \left[\frac{\left(1 - \frac{k_f}{k_p}\right)B}{\left(1 - \frac{k_f}{k_p}B\right)^2} \ln \frac{k_p}{k_f B} - \frac{B+1}{2} - \frac{B-1}{1 - \frac{k_f}{k_p}B}\right] + \sqrt{1-\epsilon}\left(\frac{k_f}{k_R} + \frac{k_f}{k_p}\right)^{-1} \quad (13)$$

where

$$\frac{k_R}{k_f} = 2.27 \times 10^{-7}\left(\frac{e}{2-e}\right)T^3\frac{d_{pv}}{k_f} \quad (14)$$

and

$$B = C\left(\frac{1-\epsilon}{\epsilon}\right)^{10/9} \quad (15)$$

with

$$C = \begin{cases} 1.25 & \text{sphere} \\ 2.5 & \text{cylinder} \\ 2.5\left[1 + \left(\frac{d_i}{d_o}\right)^2\right] & \text{hollow cylinder} \end{cases} \quad (16)$$

A comparison between the extrapolated values of the present study and the Bauer/Schlünder formula is presented in Figure 14 in the form of a parity plot. The correlations of Dixon (1988a) were used to predict void fraction for use in the correlation, as these were not measured directly in this work. Overall, there is broad agreement between theory and data, with the effect of particle conductivity being well-represented by the formula. Closer examination, however, reveals that the Bauer/Schlünder formula predicts much less variation with N than is observed in the data. The plotted points tend to lie in horizontal bands, corresponding to significant changes in observed value with N, with little predicted variation with N.

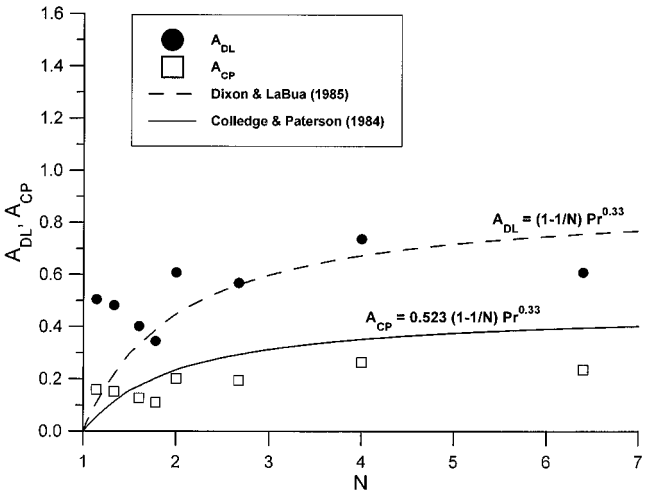

Figure 15. Comparison of the terms for the effect of N in two correlations for Nu_{wf} with data for spheres.

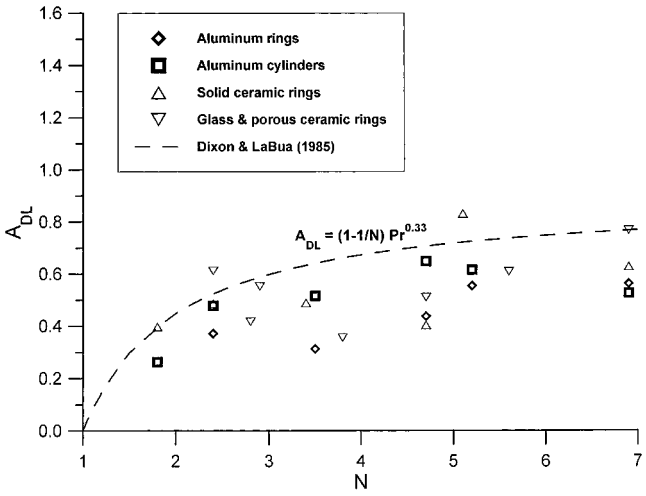

Figure 16. Comparison of the terms for the effect of N in two correlations for Nu_{wf} with data for full and hollow cylinders.

In deriving their formula, Bauer and Schlünder (1978b) claimed that wall effects on reducing conduction heat transfer would be offset by their effect on increasing radiation heat transfer. Their work was tested for $N > 10$, in which wall effects would be smaller, and in this case the good agreement they obtained between theory and data would confirm their argument. In the present work for $N < 10$, wall effects become rather large, and at the present experimental temperatures of 40−100 °C radiation is a quite small contribution, even for large particles. Even allowing for the uncertainties inherent in the extrapolation method applied to the data, we found the present results do not support Bauer and Schlünder's contention; however, it may be reasonable under higher N and higher temperature conditions.

Fluid-Phase Wall Heat Transfer Coefficient. Two formulas for Nu_{wf} have been published in recent years; both were obtained from mass transfer studies and focused on the effects of N. Colledge and Paterson (1984) found

$$Nu_{wf} = 0.523\left(1 - \frac{1}{N}\right)Pr^{1/3}Re^{0.738} = A_{CP}Re^{0.738} \qquad (17)$$

whereas Dixon and Labua (1985) obtained

$$Nu_{wf} = \left(1 - \frac{1}{N}\right)Pr^{1/3}Re^{0.61} = A_{DL}Re^{0.61} \qquad (18)$$

which are obviously in good agreement as to the influence of N, but differ in the dependence on Re. The present Nu_w data have been correlated against Re, $Re^{0.738}$, and $Re^{0.61}$. Although differences in slope and intercept were obtained, the differences in the correlation coefficient were so small as to not lead to a preference for any one of the three options.

Figure 15 shows the values obtained for A_{CP} with a correlation of Nu_w against $Re^{0.738}$ and those obtained for A_{DL} with a correlation of Nu_w against $Re^{0.61}$. The two formulas both agree with the data for spheres in Figure 15 to about the same extent, making discrimination between them difficult. Note that since both are empirical formulas and are not related to the bed-packing state, neither is able to reproduce the increase seen for $N < 2$. In Figure 16 similar results are seen with a comparison of the values of A_{DL} obtained by fitting eq 18 to data for nonspheres. Colledge and Paterson (1984) did not develop their correlation for nonspheres so a comparison would not be fair; however, the results are similar to those of Figure 15, and both formulas perform equivalently. The scatter of data seen in Figure 16 should be attributed both to experimental causes and to the use of the approximate eq 10 in fitting the Nu_w data.

Solid-Phase Wall Heat Transfer Coefficient. The intercepts at zero Re found by fitting eq 10 with Nu_{wf} given by eq 18 give values for Nu_{w0}, which were converted into wall solid Biot numbers using the Bauer/Schlünder formula for k_{rs}/k_f to avoid dividing two extrapolated quantities, by the definition $Nu_{w0} = Bi_s(k_{rs}/k_f)(2/N)$. These values derived from data were then compared to two recent formulas. The first from Martin and Nilles (1993) gives

$$Bi_s\frac{2}{N} = 1.3 + \frac{5}{N} \qquad (19)$$

while Dixon (1988b) offered

$$Bi_s\frac{2}{N} = \begin{cases} \frac{2}{N}(2.41 + 0.156(N-1)^2) & \text{spheres} \\ \frac{2}{N}(0.48 + 0.192(N-1)^2) & \text{nonspheres} \end{cases} \qquad (20)$$

The two correlations are compared to each other and to data in Figure 17, where it is clear that neither formula is clearly preferred over the other, on the basis of the data range examined here. Indeed, the data exhibit some scatter, and there is almost no dependence on N that can be discerned for the group $Bi_s(2/N)$. Further investigation will be necessary to decide this point.

Conclusions

Very strong wall effects have been observed on values of the effective radial thermal conductivity and apparent wall heat transfer coefficient estimated from data obtained in fixed beds of very low N. The high values of k_r/k_f and Nu_w that are found as N approaches unity confirm that a high degree of radial cross-flow is taking place. Systematic and potentially predictable behavior has been found for beds of spheres in the range $1 < N < 2$; however, new correlations need to be developed. The possible use of such low-N beds as single-pellet-string reactors will depend on the trade-offs among heat transfer, pressure drop, and particle diffusion limitations.

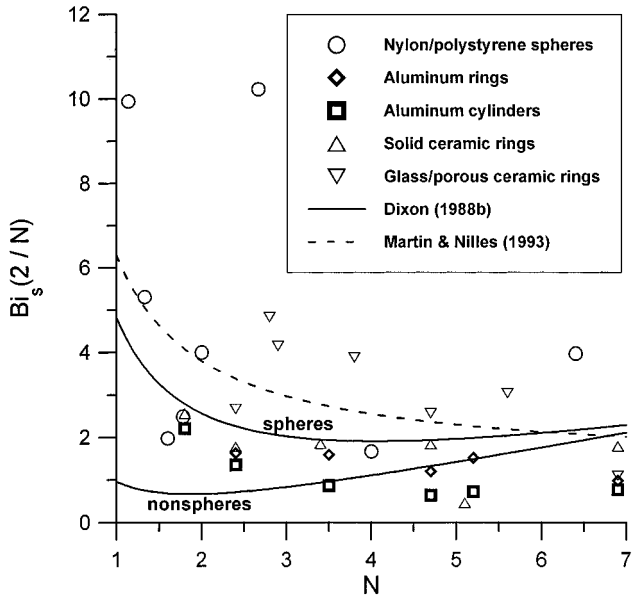

Figure 17. Comparison of two correlations for the effect of N on the solid-phase Biot number to data values extrapolated from flowing fluid data.

Current correlations for individual-phase heat transfer mechanisms are acceptable down to $N = 4$ for spheres and $N = 2$ for nonspheres. More data for $Pe_{rf}(\infty)$ will be needed to elucidate the fine structure for $2 \leq N \leq 4$ for spheres and to further investigate the region $N < 2$ for nonspheres. Data for Bi_s and k_{rs}/k_f obtained in the present study from extrapolation of flowing fluids results to $Re = 0$ were more scattered, and available correlations were in broad agreement with trends in the data. There were some indications that wall effects may influence k_{rs}/k_f more strongly than current correlations predict, especially over the lower N values and in the absence of significant radiative heat flow. Correlations for Nu_{wf} performed well over the ranges of variables studied. Data on Nu_{wf} over a wide range of Re will be needed to discriminate between correlations with different dependence on Re. In summary, many of the correlations presented by other authors performed unexpectedly well on the current data set, considering that the range of N investigated here is in many cases much lower than that for which the correlations were developed.

Acknowledgment

The author thanks Amy-Beth Brooks and Darryl Pollica for assistance in the laboratory during the performance of this work.

Nomenclature

a: specific interfacial surface area
Bi: Biot number ($h_w R/k_r$)
Bi_f: fluid-phase Biot number ($h_{wf}R/k_{rf}$)
Bi_s: solid-phase Biot number ($h_{ws}R/k_{rs}$)
c_p: specific heat of gas
d_{pv}: diameter of sphere of equivalent volume to particle
d_t: diameter of tube
e: emissivity of the packing
G: superficial gas axial flow rate/area
h: apparent fluid-to-solid heat transfer coefficient
h_w: apparent wall heat transfer coefficient
h_{wf}: apparent wall-to-fluid heat transfer coefficient
h_{ws}: apparent wall-to-solid heat transfer coefficient
k_a: effective axial thermal conductivity
k_{as}: solid-phase effective axial thermal conductivity
k_f: fluid thermal conductivity
k_p: particle thermal conductivity
k_r: effective radial thermal conductivity
k_r^0: effective radial thermal conductivity under stagnant ($Re = 0$) conditions
k_{rf}: fluid-phase effective radial thermal conductivity
k_{rs}: solid-phase effective radial thermal conductivity
k_R: radiation conductivity
N: tube-to-particle diameter ratio
N_s: dimensionless interphase heat transfer coefficient ($ad_t^2h/4k_{rs}$)
Nu_w: wall Nusselt number ($h_w d_p/k_f$)
Nu_{wf}: wall-to-fluid Nusselt number ($h_{wf}d_p/k_f$)
Pe_a: axial Peclet number ($Gc_p d_p/k_a$)
Pe_r: radial Peclet number ($Gc_p d_p/k_r$)
Pe_{rf}: fluid-phase radial Peclet number ($Gc_p d_p/k_{rf}$)
$Pe_{rf}(\infty)$: limiting $Re \rightarrow \infty$ fluid-phase radial Peclet number ($Gc_p d_p/k_{rf}$)
Pr: Prandtl number ($\mu c_p/k_f$)
R: radius of tube
Re: particle Reynolds number (Gd_p/μ)
r: radial coordinate
T: measured temperature
T_0: inlet gas temperature to fixed bed
T_w: wall temperature of fixed bed
v: superficial gas velocity in tube
x: dimensionless axial coordinate (z/R)
y: dimensionless radial coordinate (r/R)
z: axial coordinate

Greek Symbols

μ: viscosity of gas phase
θ: dimensionless temperature ($(T - T_0)/(T_w - T_0)$)
θ_{wc}: dimensionless wall temperature ($(T_{wc} - T_0)/(T_w - T_0)$)

Literature Cited

Ahn, B.; Zoulalian, A.; Smith, J. M. Axial Dispersion in Packed Beds with Large Wall Effects. *AIChE J.* **1986**, *32*, 170−174.

Bauer, R.; Schünder, E. U. Effective Radial Thermal Conductivity of Packings in Gas Flow. Part I Convective Transport Coefficient. *Int. Chem. Eng.* **1978a**, *18*, 181−188.

Bauer, R.; Schlünder, E. U. Effective Radial Thermal Conductivity of Packings in Gas Flow. Part II Thermal Conductivity of the Packing Fraction Without Gas Flow. *Int. Chem. Eng.* **1978b**, *18*, 189−204.

Benenati, R. F.; Brosilow, C. B. Void Fraction Distribution in Beds of Spheres. *AIChE J.* **1962**, *8*, 359−361.

Borkink, J. G. H.; Borman, P. C.; Westerterp, K. R. Modeling of Radial Heat Transport in Packed Beds - Confidence Intervals of Estimated Parameters and Choice of Boundary Conditions. *Chem. Eng. Commun.* **1993**, *99*, 135−155.

Chalbi, M.; Castro, J. A.; Rodrigues, A. E.; Zoulalian, A. Heat Transfer Parameters in Fixed Bed Exchangers. *Chem. Eng. J.* **1987**, *34*, 89−97.

Chu, C. F.; Ng, K. M. Flow in Packed Tubes with a Small Tube to Particle Diameter Ratio. *AIChE J.* **1989**, *35*, 148−158.

Colledge, R. A.; Paterson, W. R. Heat Transfer at the Wall of a Packed Bed: A j-Factor Analogy Established. In *Collected Papers*; 11th Annual Research Meeting; Institution of Chemical Engineers: Bath, 1984; 6 pages.

Cresswell, D. L. Heat Transfer in Packed Bed Reactors. In *Chemical Reactor Design and Technology*, NATO Series E No. 110; de Lasa, H. I., Ed.; Martinus Nijhoff: Dordrecht, 1986; pp 687−728.

DeWasch, A. P.; Froment, G. F. Heat Transfer in Packed Beds. *Chem. Eng. Sci.* **1972**, *27*, 567−576.

Dixon, A. G. The Length Effect on Packed Bed Effective Heat Transfer Parameters. *Chem. Eng. J.* **1985**, *31*, 163−173.

Dixon, A. G. Correlations for Wall and Particle Shape Effects on Fixed Bed Bulk Voidage. *Can. J. Chem. Eng.* **1988a**, *66*, 705−708.

Dixon, A. G. Wall and Particle-Shape Effects on Heat Transfer in Packed Beds. *Chem. Eng. Commun.* **1988b**, *71*, 217−237.

Dixon, A. G. Angular Temperature Variations in Fixed Beds of Spheres. In *HTD-236*; 29th National Heat Transfer Conference; ASME: Atlanta, 1993; pp 55−64.

Dixon, A. G. Heat Transfer in Packed Beds of Spheres with $D_T/D_P \leq 4$. In *Proceedings of the 10th International Heat Transfer Conference*; Hemisphere: Brighton, U.K., 1994; Vol. 5, pp 225−230.

Dixon, A. G.; Cresswell, D. L. Theoretical Prediction of Effective Heat Transfer Parameters in Packed Beds. *AIChE J.* **1979**, *25*, 663−676.

Dixon, A. G.; LaBua, L. A. Wall-to-Fluid Coefficients for Fixed Bed Heat and Mass Transfer. *Int. J. Heat Mass Transfer* **1985**, *28*, 879−881.

Dixon, A. G.; Yoo, C. Heat Transfer in Packed Beds of Very Low Tube-to-Particle Diameter Ratio. In *Heat and Mass Transfer in Porous Media*; Quintard, M., Todorovic, M., Eds.; Elsevier: Amsterdam, 1992; pp 573−584.

Fahien, R. W.; Smith, J. M. Mass Transfer in Packed Beds. *AIChE J.* **1955**, *1*, 28−37.

Govindarao, V. M. H.; Froment, G. F. Voidage Profiles in Packed Beds of Spheres. *Chem. Eng. Sci.* **1986**, *41*, 533−539.

Govindarao, V. M. H.; Ramrao, K. V. S.; Rao, A. V. S. Structural Characteristics of Packed Beds of Low Aspect Ratio. *Chem. Eng. Sci.* **1992**, *47*, 2105−2109.

Hsiang, T. C.; Haynes, H. W., Jr. Axial Dispersion in Small Diameter Beds of Large Spherical Particles. *Chem. Eng. Sci.* **1977**, *32*, 678−681.

Kershenbaum, L. S.; Lopez-Isunza, F. Dynamic Behavior of an Industrial Scale Fixed-Bed Catalytic Reactor. *ACS Symp. Ser.* **1982**, *196*, 109−120.

Kunii, D.; Suzuki, M.; Ono, N. Heat Transfer from Wall Surface to Packed Beds at High Reynolds Number. *J. Chem. Eng. Jpn.* **1968**, *1*, 21−26.

Martin, H.; Nilles, M. Radiale Wärmeleitung in Durchströmten Schuttüngsrohren. *Chem.-Ing.-Tech.* **1993**, *65*, 1468−1477.

McGreavy, C.; Foumeny, E. A.; Javed, K. H. Characterization of Transport Properties for Fixed Beds in Terms of Local Bed Structure and Flow Distribution. *Chem. Eng. Sci.* **1986**, *41*, 787−797.

Mongkhonsi, T.; Lopez-Isunza, H. F.; Kershenbaum, L. S. The Distortion of Measured Temperature Profiles in Fixed-Bed Reactors. *Trans. Inst. Chem. Eng.* **1992**, *70A*, 255−264.

Mueller, G. E. Radial Void Fraction Distributions in Randomly Packed Fixed Beds of Uniformly Sized Spheres in Cylindrical Containers. *Powder Technol.* **1992**, *72*, 269−275.

Mueller, G. E. Angular Void Fraction Distributions in Randomly Packed Fixed Beds of Uniformly Sized Spheres in Cylindrical Containers. *Powder Technol.* **1993**, *77*, 313−319.

Olbrich, W. E.; Potter, O. E. Heat Transfer in Small Diameter Packed Beds. *Chem. Eng. Sci.* **1972a**, *27*, 1723−1732.

Olbrich, W. E.; Potter, O. E. Mass Transfer from the Wall in Small Diameter Packed Beds. *Chem. Eng. Sci.* **1972b**, *27*, 1733−1743.

Rao, S. M.; Toor, H. L. Heat Transfer Between Particles in Packed Beds. *Ind. Eng. Chem. Fundam.* **1984**, *23*, 294−298.

Scott, D. S.; Lee, W.; Papa, J. The Measurement of Transport Coefficients in Gas-Solid Heterogeneous Reactions. *Chem. Eng. Sci.* **1974**, *29*, 2155−2167.

Solcova, O.; Schneider, P. Axial Dispersion in Single-Pellet-String Columns Packed with Cylindrical Particles. *Chem. Eng. Sci.* **1994**, *49*, 401−408.

Vortmeyer, D.; Winter, R. P. On the Validity Limits of Packed Bed Reactor Continuum Models with Respect to Tube to Particle Diameter Ratio. *Chem. Eng. Sci.* **1984**, *39*, 1430−1432.

Received for review September 30, 1996
Revised manuscript received February 5, 1997
Accepted February 7, 1997[⊗]

IE9605950

[⊗] Abstract published in *Advance ACS Abstracts,* June 15, 1997.